INTERNATIONAL JOURNAL FOR NUMERICAL AND ANALYTICAL METHODS IN GEOMECHANICS
Int. J. Numer. Anal. Meth. Geomech., **23**, 1075–1100 (1999)

MICROMECHANICS MODEL FOR ELASTIC STIFFNESS OF NON-SPHERICAL GRANULAR ASSEMBLY

J.-J. DONG AND Y.-W. PAN*

Department of Civil Engineering, National Chiao-Tung University, Hsinchu 30010, Taiwan, ROC

SUMMARY

This paper presents a micromechanics model for the elastic stiffness of a non-spherical granular assembly. The microstructural continuum model of ideal spherical assembly is extended for non-ideal assembly. The presented work takes the effects of gradation, shape, and preferred orientation into account by introducing a directional distribution function of branch-vector length. The microstructure of a granular assembly is described by the distributions of packing structure, branch-vector length, and particle number per unit volume. These distributions account or the random nature of a realistic granular material. The microfeatures relevant to the description of non-deal particle assembly are elaborated. The influences of various direction-dependent and direction-independent microfeatures on the elastic stiffness are demonstrated. Hypothetical non-ideal granular assemblies are used to study the effects of gradation, shape and preferred orientation. Based on the proposed model, the paper discusses the inherent anisotropy in a non-ideal granular assembly. The presented work also makes use of a generalized static hypothesis to estimate the contact-force distribution for specific microstructure and stress state. With the estimated contact-force and the Hertz–Mindlin contact theory, the elastic stiffness of a particulate assembly can be evaluated. Hence, the effects of geometric fabric and anisotropic stress state on the elastic stiffness can be deliberated. Consequently, the effects of geometric fabric and kinetic fabric of a natural granular material can be evaluated independently. It is shown that the proposed model can reasonably capture the phenomena of inherent anisotropy and stress-induced anisotropy of a non-spherical granular assembly under small strain.

KEY WORDS: micromechanics model; granular assembly; elastic stiffness; fabric; inherent anisotropy; stress-induced anisotropy

INTRODUCTION

For the last two decades, many researchers have used micromechanics to study the mechanical behaviours of granular materials from the microscopic view. In general, two types of micromechanics approach have been widely used. Numerical simulation approach, such as the discrete-element method[1–4] or the discontinuous deformation analysis,[5] takes particle interaction into account explicitly by treating contact mechanisms numerically. The microstructural continuum approach on the other hand, formulates the stress–strain relationship implicitly by

* Correspondence to: Y.-W. Pan, Department of Civil Engineering, National Chiao-Tung University, Hsinchu 30010, Taiwan, ROC.

Contract grant sponsor: National Science Council, Republic of China

CCC 0363–9061/99/111075–26$17.50
Received 22 October 1997
Revised 9 November 1998

averaging over the microfeatures of granular assembly.[6–9] The numerical approach is only appropriate for simulating laboratory experimental result with relatively limited particle number and boundary conditions. For solving practical engineering problems with numerous particles, this approach becomes very ineffective and is rarely used. Relatively, the microstructural continuum approach seems more appropriate for engineering applications.

The theoretical basis of microstructural continuum approach has become increasingly solid owing to the efforts devoted to granular materials from microscope view by the pioneers in various research fields. One of the fundamental works for simulating the global stress–stain relationship by micromechanics is to link the global variables (e.g. stress or strain) with local variables (e.g. contact force or relative contact displacement) in a concerned scale.[10,11] The energy conservation principle and equilibrium condition can be adopted to derive the localized relative contact displacement in terms of strain and averaged stress with respect to contact force, respectively.[9] The uniform strain theory[12] and the principle of virtual work[6] are also effective for deriving similar relationships. Consequently, the global constitutive law of a randomly packing granular assembly can be derived in terms of microfeatures with a specified local constitutive law.[13]

Recently, more rigorous homogenization processes are developed for deriving the global constitutive law. Three homogenization processes (defined as the process 0, 1 and 2, respectively) are proposed by Emeriault and Cambou[11] using three different averaging and localization operators. In an independent study, Chang *et al.*[14] derive the upper bound and the lower estimate, respectively, of the elastic constants of an ideal assembly (with mono-size spheres) through the static and kinematic hypothesis, respectively. The kinematic hypothesis corresponds to the strain localization, and the static hypothesis corresponds to the stress localization. Figure 1 illustrates the framework and hypothesis for deriving the upper bound and the lower estimate of the initial elastic constants proposed by Chang *et al.*[14]

Some limitations still exist for applying the micromechanics model to engineering practice in spite of the sound theoretical background. First, it is difficult to experimentally determine the microstructure of a granular material. The development of the technique for measuring microstructure of ranular materials in laboratory or *in situ* experimentally is far behind the development of micromechanics theory. Pan and Dong[15] presents a methodology for evaluating the

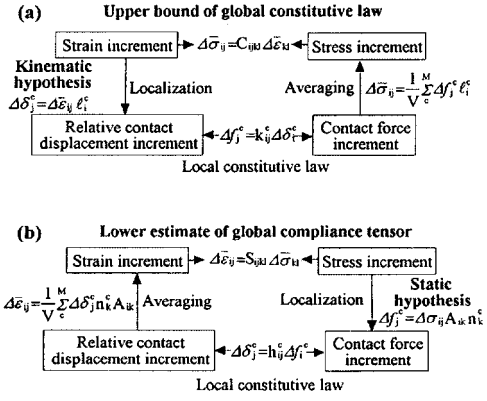

Figure 1. Framework and hypothesis of microstructural continuum approach: (a) upper bound; and (b) lower estimate

geometric fabric of granular assembly from measured wave velocity. The enhancement of the fabric characterization of natural granular material can make the microstructural continuum model more attractive and applicable. Secondly, most of the micromechanics models assume that the granular assembly is composed of equal-sized spherical particles. However, naturally deposited granular materials are rarely mono-sized and spherically shaped. Due to the consequence of deposition, a natural granular deposit tends to form a packing structure with more contact normally distributed in the vertical direction.[16] Also, the long-axis of non-spherical granular particles in a natural deposit tends to align in the orientation of horizontal plane. The micromechanics models for ideal assembly may miss the true fabric nature and fail to characterize the microstructure of a natural deposit.

Very few researchers have studied the micromechanics of a granular assembly containing non-spherical particles. Rothenburg and Bathurst[3] as well as Ng[4] use the discrete-element stimulation to study the mechanical behaviour of the two-dimensional granular assemblies composed of planar ellipitcal particles. The influences of particle's shape and preferred orientation on the mechanical behaviour of natural granular materials appear predominant. The effects of shape and orientation also result in a certain degree of inherent anisotropy.[17] Thus, the microstructure (also termed 'geometric fabric') of naturally formed granular materials involved in a micromechanics-based model should include the distribution of branch-vector length (i.e. the distance between the two adjacent particles' centroids) in order to account for the preferred orientation of particles.

In this paper, the microstructural continuum model of the ideal assembly[7] is extended for non-ideal assemblies. The microstructure of the granular assembly includes the distributions of packing structure, branch-vector length, and particle number per unit volume. They are represented by statistical expressions. The presented work implicitly takes effects of gradation, shape and preferred orientation into account by a direction-dependent function of branch-vector length distribution. Along with the contact normal distribution, the particles' shapes and orientations affect the inherent anisotropy of a non-spherical granular assembly. In addition to the effect of microstructure, the effect of anisotropic stress state on the elastic stiffness is also elaborated. A generalized static hypothesis is proposed to estimate the distribution of averaged contact-forces magnitude in various direction (termed 'kinetic fabric', as defined by Chen *et al.*[18]). Consequently, the inherent anisotropy and the stress-induced anisotropy (a kind of the 'induced anisotropy') of a natural granular material under small strain can be evaluated independently.

MICROMECHANICS ELASTIC MODEL OF GRANULAR ASSEMBLY

Model for ideal granular assembly

The microstructural continuum approach can be used to model the macroscopic mechanical behaviours of a randomly packing granular assembly.[7] One can derive the homogenized (averaged) constitutive law by combining the local constitutive law and the relations between the averaged and local features of granular assembly in a representative volume. A complete stress–strain curve of granular materials can be simulated incrementally through the homogenization process as long as the microstructure and its evolution can be updated reasonably.[19,20] The microstructure evolution (accompanied with particle sliding, separation, and rotation) may result in the non-linear behaviour of granular materials under large strain. The microstructure of granular materials changes negligibly if the strain is small (e.g. 10^{-5}–10^{-6}). Hence, the initial

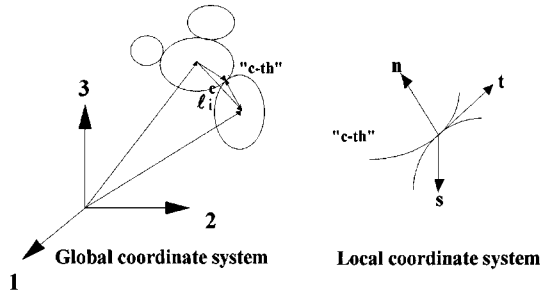

Figure 2. The global and local coordinate system

elastic stiffness tensor of granular assembly can be derived assuming an unchanged microstructure under low strain.

Chang[7] derives the general form of granular assembly's stiffness tensor as follows:

$$C_{ijkl} = \frac{1}{V} \sum_{c=1}^{M} \ell_i^c \cdot k_{jl}^c \cdot \ell_k^c \tag{1}$$

where V is the representative volume of the granular assembly, M is the total contact number in the volume V, $\ell_i^c = \ell^c \cdot n_i^{\ell^c}$ is the branch vector in which ℓ^c is the length of the cth branch vector; $n_i^{\ell^c}$ is the unit branch vector at the cth contact; and k_{jl}^c is the transformed contact stiffness tensor at the cth contact on the global co-ordinate.

The transformed contact stiffness tensor, k_{jl}^c, is a function of the local contact stiffnesses as follows:

$$k_{jl}^c = k_n^c \cdot n_j^c \cdot n_l^c + k_s^c \cdot s_j^c \cdot s_l^c + k_t^c \cdot t_j^c \cdot t_l^c \tag{2}$$

in which k_n^c , k_s^c and k_t^c, respectively, are the constant stiffnesses along the direction of n_j^c, s_j^c and t_j^c, respectively. The three orthrotropic unit vectors n_j^c, s_j^c and t_j^c, shown in Figure 2, define the local co-ordinate system at the contact point. A discussion of the contact stiffness will appear in the latter part of the paper.

For an ideal assembly, the unit contact normal n_j^c and the unit branch vector $n_i^{\ell^c}$ are identical; and the branch-vector length ℓ^c is twice of the sphere radius. As a result, the homogenized stiffness tensor of an ideal assembly has the following form:

$$C_{ijkl} = \frac{4 \cdot r^2}{V} \sum_{c=1}^{M} n_i^c \cdot k_{jl}^c \, n_k^c \tag{3}$$

where r is the particle radius.

For a representative volume with a lost of contacts, a continuous density function $E(\tilde{n})$ can be introduced in equation (3) to account for the random variation of contact-normal directions in the volume. The contact-normal density function $E(\tilde{n})$ defines the contact density along the $\tilde{n}(= n_i)$ direction among total contacts. $E(\tilde{n})$ can be expressed as $E(\tilde{n}) = N^{\tilde{n}}/2M$ in which $N^{\tilde{n}}$ is the total contact number along the $\tilde{n}$ direction. Rewriting equation (3) in an integral form and including $E(\tilde{n})$, one can obtain the following expression:

$$C_{ijkl} = \frac{1}{2} \frac{(4r^2)}{V} (2 \cdot M) \int_{\Omega} n_i^c \cdot k_{jl}^c \cdot n_k^c \cdot E(\tilde{n}) \, \mathrm{d}\Omega. \tag{4}$$

In the above equation, $\int_\Omega (\cdot)\cdot E(\tilde{n})\,\mathrm{d}\Omega = \int_0^\pi \int_0^{2\pi} (\cdot)\cdot E(\alpha,\beta)\cdot \sin\beta\,\mathrm{d}\alpha\,\mathrm{d}\beta$, $\mathrm{d}\Omega$ denotes an elementary angle equal to $\sin\beta\,\mathrm{d}\alpha\,\mathrm{d}\beta$; and Ω is the unit sphere defined by $0 \leqslant \alpha < 2\pi$, $0 \leqslant \beta < \pi$. The density function $E(\tilde{n})$ is centro-symmetric.

Assuming a linear local constitutive law, Chang and Misra[13] adopted the kinematics hypothesis to derive a closed-form solution of equation (4) for randomly packing assemblies. Their homogenized stiffness tensor is an upper bound solution. Recently, Chang *et al.*[14] derived a lower estimate of elastic tensor in an analytical form under the static hypothesis.

Extended model for non-ideal granular assembly

Naturally deposited granular materials are seldom mono-sized and spherical. Only limited researchers[3,4,21] have studied the mechanical behaviour of two dimensional granular assemblies composed of planar elliptical particles. The influence of particle's shape and orientation on the mechanical behaviour of natural granular materials appear predominant. Using statistical approach, Oda *et al.*[22] studied the microstructure of random assemblies composed of graded spherical particle. They suggested a density function to estimate the distribution of the branch lengths in terms of the particle-size distribution. Moreover, the microstructure of an assembly composed of graded non-spherical particles is far more complicated. By introducing statistical fabric distributions, the foregoing elastic stiffness of an ideal assembly will be extended to model the materials composed of graded and non-spherical particles.

The branch-vector lengths in equation (1) are no more constant for a graded, non-spherical particles' assembly. To account for the effects of gradation, shape and preferred orientation, the summation in equation (1) over contacts (from 1 to M) in the representative, volume should be replaced by summing over each direction of contact normal and each length of branch vector. Let us divide all the directions of contact normal into P sets and divide all the branch-vector lengths along each $\tilde{n}^a$ direction into Q^a sets. Equation (1) can be expressed in the following summation form:

$$C_{ijkl} = \frac{1}{V}\left(\sum_{a=1}^{P} \left\{ \sum_{1}^{Q^a} N_\ell^{\tilde{n}^a} \cdot [\ell\cdot(n_p)^a] \cdot k_{jl}^a(\ell) \cdot [\ell\cdot(n_q)^a] \cdot r_{pqik} \right\} \right) \tag{5}$$

In the above equation, $N_\ell^{\tilde{n}^a}$ is the contact number along the $\tilde{n}^a$ direction with a branch-vector length equal to ℓ. The deviation tensor r_{pqik} accounts for the deviation of branch vector and the contact-normal directions for a non-spherical granular assembly, it satisfies the condition $n_i^{\ell}\cdot n_k^{\ell} = r_{pqik}\cdot n_p \cdot n_q$. In addition to $E(\tilde{n})$ which is defined previously, a density function $g^{\tilde{n}}(\ell) = N_\ell^{\tilde{n}}/N^{\tilde{n}}$ can be introduced in which $N^{\tilde{n}^a}$ is the contact number along the $\tilde{n}^a$ direction. The function $E(\tilde{n})$ is the contact-normal density function. The function $g^{\tilde{n}}(\ell)$ is the distribution function of branch-vector length. Consequently, equation (5) can be formulated in an integral form as follows:

$$C_{ijkl} = \frac{1}{2}\left(\frac{2\cdot M}{V}\right)\cdot \left\{ \iiint_\Omega \left[\int_\ell g^{\tilde{n}}(\ell)\cdot \ell^2 \cdot n_p \cdot k_{jl}\cdot n_q \cdot r_{pqik}\,\mathrm{d}\ell \right] \cdot E(\tilde{n})\,\mathrm{d}\Omega \right\} \tag{6}$$

The branch-vector length distribution function $g^{\tilde{n}}(\ell)$ implicitly reflects the effects of gradation, shape and preferred orientation; it also accounts for the orientation of particles. The integration of branch-vector length over ℓ enables the consideration of branch-vector length fluctuation. Clearly, the function $g^{\tilde{n}}(\ell)$ must be direction dependent for a randomly distributed non-ideal granular assembly. A Fourier series expansion can describe the two-dimensional directional data.

Similarly, a spherical harmonics expansion, works for three-dimensional directional data. Fabric tensor,[23] i.e. the polynomial expansion of the unit vector, is an another way of expression. In literature the ways for describing contact-normal distribution has extensively been discussed.[13,23–25] A discussion on the representation of branch-vector length distribution function $g^{\tilde{n}}(\ell)$ will appear in the next section.

Equation (6) takes into account the gradation and orientation effects on the elastic behaviour of a graded and non-spherical granular assembly. If the deviation between the contact-normal and branch vector is neglected (i.e. assuming that the contact normal and the branch vectors are collinear, or $r_{pqik} = I_{pqik}$), equation (6) reduces to

$$C_{ijkl} = \frac{1}{2}\left(\frac{2 \cdot M}{V}\right) \cdot \left\{ \iint_{\Omega} \left[\int_{\ell} g^{\tilde{n}}(\ell) \cdot \ell^2 \cdot n_i \cdot k_{jl} \cdot n_k \, \mathrm{d}\ell \right] \cdot E(\tilde{n}) \, \mathrm{d}\Omega \right\}. \tag{7}$$

For an uniform spherical granular assembly, the branch-vector length is unique. Thus, equation (7) further reduces to equation (4).

STATISTICAL DESCRIPTION OF MICROSTRUCTURE OF A NON-IDEAL GRANULAR ASSEMBLY

From equation (6), the effects of gradation, shape, and preferred orientation of natural granular materials on the elastic stiffness tensor mainly arises from (1) the total contact number per unit volume M/V, (2) the distribution function of branch-vector length $g^{\tilde{n}}(\ell)$, and (3) the deviation tensor r_{pqik}. These items are discussed in the following context, separately.

The total contact number per unit volume M/V

Oda *et al.*[22] express the total contact number per unit volume M/V by the following equation:

$$\frac{M}{V} = \frac{P^v}{V} \cdot \frac{M}{P^v} = \delta^v \cdot \frac{\bar{N}^t}{2} \tag{8}$$

where P^v is the total particle number in the volume V, δ^v is the total particle number per unit volume, and $\bar{N}^t$ is he average co-ordination number. Oda[26] shows that $\bar{N}^t$ does not depend on the grain-size distribution. Experimental data also shows that the average co-ordination number $\bar{N}^t$ has a good correlation with void ratio e.[26] Many empirical equations are proposed to correlate e with $\bar{N}^t$.[26,27]

The particle number per unit volume δ^v is

$$\delta^v = \frac{P^v}{(1 + e) \cdot V_s} \tag{9}$$

where V_s is the volume of solid. The microfeatures, including particle's packing, gradation, shape, and preferred orientation determine the void ratio of a granular assembly. The volume of solid V_s can be calculated by integrating over the production of (i) the volume of a particle with the size r, (ii) the total particle number, and (iii) the size density function. Thus, this integration yields

$$V_s = \int_{r_m}^{r_M} v_s(r) \cdot P^v \cdot f^p(r) \cdot \mathrm{d}r, \tag{10}$$

where r_m and r_M, respectively, are the minimum and maximum of particle radius, respectively; $v_s(r)$ is the volume of a particle with the size r; $f^p(r)$ is the size density function satisfying $\int_{r_m}^{r_M} f^p(r)\,dr = 1$. The size density function $f^p(r)$ accounts for the gradation effect in a non-uniform sized assembly.[22]

For an arbitrarily shaped particle, one may consider an equivalent spherical particle with the same volume. An equivalent radius r_e satisfying $v_s(r_e) = \frac{4}{3} \cdot \pi \cdot r_e^3$, is defined. Using the equivalent radius, the particle number per unit volume δ^v yields the following form:

$$\delta^v = \frac{1}{(1+e) \cdot \int_{r_m}^{r_M} (\frac{4}{3} \cdot \pi \cdot r_e^3) \cdot f^p(r_e)\,dr_e} \tag{11}$$

where $f^p(r_e)$ is the modified size density function for a non-spherical granular assembly. With equation (11), the parameter δ^v can take the effects of gradation and shape into account.

The formulation of $f^p(r)$ and $f^p(r_e)$ follows. The (particle-) size density function $f^p(r)$ in equation (10) is direction independent. For a spherical granular assembly, $f^p(r)$ can be derived from the (particle-) size density function by volume $f^v(r)$ as follows:

$$f^p(r) = \frac{f^v(r)/r^3}{\int_{r_m}^{r_M} f^v(r)\,dr/r^3} \tag{12}$$

By integrating $f^v(r)$ over r, the gradation function $F(r)$ represents the particle-size-distribution curve of natural granular materials.

$$F(r) = \int_{r_m}^{r} f^v(r)\,dr \tag{13}$$

The density function $f^v(r)$ and the gradation function $F(r)$ are usually expressed as functions of particle diameter ρ instead of radius r. A conversion can be made by $F(\rho) = F(r)$ and $f^v(\rho) = f^v(r)/2$. Feda[28] presented analytical expression of $f^v(r)$ of natural granular materials by adopting the normal distribution, log-normal distribution or semi-empirical formulas. Each different distribution function will simulate a different type of gradation curve for a material formed in a different genetic process.

For a non-spherical granular assembly,the equivalent size density function of $f^p(r_e)$ in equation (11) can be deduced from the gradation curve with a modification on particle sizes. A gradation curve correlates the accumulated volume faction to the particle size in the shortest dimension. Feda[28] estimated this grain size by multiplying the equivalent diameter $\rho_e (= 2r_e)$ by a reduction coefficient dependent on particle shape.[29] The conversion of mass fraction into volume fraction for a gradation curve has no problem as long as the specific gravity of the granular material is known. As a result, one can easily derive the equivalent size density function $f^p(r_e)$ from the gradation curve of a natural granular material.

The distribution function of branch-vector-length $g^{\tilde{n}}(\ell)$

The function $g^{\tilde{n}}(\ell)$ represents the variation of the branch-vector length in various directions. This function depends on the particle size, shape and orientation. For a spherical particle assembly, $g^{\tilde{n}}(\ell)$ is directly related to a function of the material's gradation curve. For a non-spherical particle assembly, $g^{\tilde{n}}(\ell)$ can be represented by combining a direction-independent distribution function $g(\ell)$ and a direction-dependent weighting function $W(\tilde{n})$, as follows:

$$g^{\tilde{n}}(\ell) = g(\ell) \otimes W(\tilde{n}) \tag{14}$$

where $(\cdot) \otimes (\cdot)$ denotes a certain form of mathematical operation. For an isotropic branch-vector length distribution ($W(\tilde{n}) = 1$), equation (14) can reduce to

$$g^{\tilde{n}}(\ell) = g(\ell) \tag{15}$$

Taking the total particle contacts in a granular assembly as the statistical sample, a distribution function of branch-vector length $g^{\text{total}}(\ell)$ can be evaluated. This distribution function is direction independent and can be calculated from the size density function $f^p(r)$.[22]

$$g^{\text{total}}(\ell) = \frac{\int_{\ell - r_m}^{\ell - r_M} f^p(r) \cdot f^p(\ell - r)\, \mathrm{d}r}{\int_{2r_m}^{2r_M} \int_{\ell - r_m}^{\ell - r_M} f^p(r) \cdot f^p(\ell - r)\, \mathrm{d}r\, \mathrm{d}l} \tag{16}$$

Using equations (12), (13) and (16), one can derive $g^{\text{total}}(\ell)$ from the gradation curve of a granular assembly.

The term $g^{\tilde{n}}(\ell)$ represents a distribution function of the branch-vector length in a specific direction $\tilde{n}$. Hence, the statistical sample represents all the branch vectors in the $\tilde{n}$ direction. If the branch-vector length distributes equally in all directions, the branch-vector length distribution function $g^{\tilde{n}}(\ell) = g(\ell)$ can be approximated by the following equation:

$$g(\ell) = \frac{[g^{\text{total}}(\ell)]^{1/3}}{\int [g^{\text{total}}(\ell)]^{1/3}\, \mathrm{d}\ell} \tag{17}$$

For a long-normal distribution function $f^v(r)$ such as

$$f^v(r) = \frac{A}{\log(s_r) \cdot \sqrt{2\pi}} \cdot \exp\left\{ - \frac{[\log(r) - \log(r_{50})]^2}{2[\log(s_r)]^2} \right\} \tag{18}$$

the function $g(\ell)$ remains a long-normal distribution function as follows:

$$g(\ell) = \frac{A}{\log(s_\ell) \cdot \sqrt{2\pi}} \cdot \exp\left\{ - \frac{[\log(\ell) - \log(\ell_{50})]^2}{2[\log(s_\ell)]^2} \right\} \tag{19}$$

where A and A' are constants satisfying $\int f^v(r)\, \mathrm{d}r = \int g(\ell)\, \mathrm{d}l = 1$, r_{50} and ℓ_{50} are the sample means, s_r and s_ℓ are the standard deviations of $f^v(r)$ and $g(\ell)$ calculated for hypothetical granular assemblies of long-normal distributed $f^v(r)$ are presented. Table I lists the r_{50} and s_r for each hypothetical granular assembly. Six distribution curves calculated from equation (13) are shown in Figure 3. Figure 4 shows the calculated curves of $f^p(r)$, $g^{\text{total}}(\ell)$, and $g(\ell)$ with the curve numbered in Figure 3.

Due to the process of natural deposition, the branch-vector length distribution along various directions can be different. Oda *et al.*[22] discussed branch-vector length distribution only for isotropic distributed spherical particulate assembly. So far, the influence of geometric fabric on the elastic constants for non-spherical assembly was only studied by means of numerical stimulation.[3,4] It is also possible to investigate this problem using the extended model, equations (6) and (7), incorporating a statistical representation of equation (14).

The distribution of the branch-vector length $g^{\tilde{n}}(\ell)$ can be described by a direction-dependent density function such as equation (14). A possible form of equation (14) is to introduce a direction-dependent $\ell_{50}^{\tilde{n}}$ and $s_\ell^{\tilde{n}}$ into equation (19), $\ell_{50}^{\tilde{n}}$ and $s_\ell^{\tilde{n}}$ are the ℓ_{50} and s_ℓ, respectively, along the direction $\tilde{n}$. Both a preferred orientation of non-spherical particles and a directionally distributed gradation may result in the dependency of $\ell_{50}^{\tilde{n}}$ on direction. The direction-dependent $s_\ell^{\tilde{n}}$ reflects the variation of branch-vector length in the various direction arising from gradation. Both the

Table I. Sample mean and standard deviation of hypothetical granular assemblies in Figure 3

Curves in Figure 3	1	2	3	4	5	6
Mean size r_{50}	10 mm	2 mm	1 mm	5 mm	5 mm	5 mm
Standard deviation of size s_r (C_u)	1·5(1·9)	1·5(1·9)	1·5(1·9)	2·0(2·9)	1·5(1·9)	1·2(1·3)

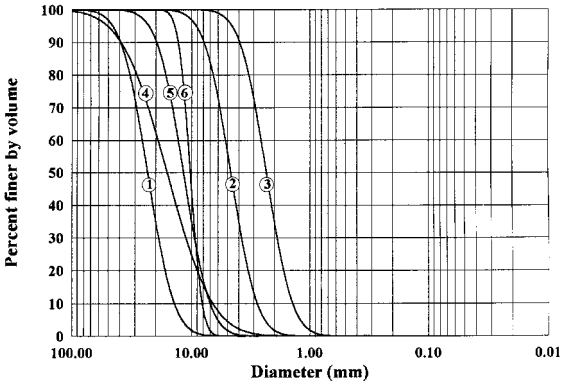

Figure 3. Gradation curve of hypothetical granular assemblies

sample mean and the standard deviation of branch-vector length distribution function are independent of direction if the particles' gradation and orientation are uniformly distributed.

The deviation tensor r_{pqik}

For a non-spherical particle assembly, the directions of contact normal and branch-vector are different. Their deviation is due to the shape and orientation of non-spherical particles. The deviation tensor r_{pqik} in equation (6) accounts for this effects of shape and orientation. However, it is very difficult (if not possible) to evaluate r_{pqik} analytically or quantitatively due to the random nature of particle shapes and orientation. Microscopic observation and numerical simulation may be the possible means for exploring this problem. Rothernburg and Bathurst[3] formulated the stress homogenization (averaging over the contact forces) of a bi-axially loaded elliptical particulate assembly. In their formulation, the deviation between the contact normal and the contact vector (i.e. the vector connecting the contact point and the particle centroid) is neglected. They found that the discrepancy between the DEM simulated results and the calculated results of stress is negligible before failure. The effect of r_{pqik} on the elastic stiffness tensor needs further investigation. However, the presented study does not attempt to explore this aspect in detail. In the latter parametric study, we are going to assume $r_{pqik} = I_{pqik}$ (i.e. the collinear of contact normal and branch vectors) for the sake of convenience. Rothenburg nd Bathurst[3] data supports the adequacy for assuming $r_{pqik} = I_{pqik}$ in a small strain condition. It should be pointed out that, only under this assumption, equation (6) can reduce to equation (7). The collinear assumption is not required in the extended model if one adopts equation (6) instead of equation (7) with a determined r_{pqik} for a non-spherical particulate assembly.

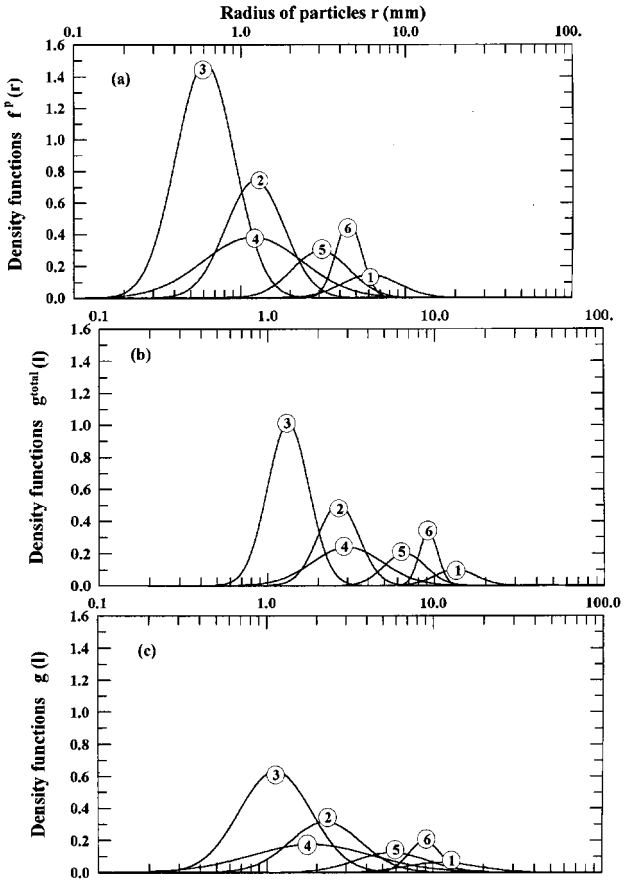

Figure 4. Density functions of hypothetical granular assemblies in Figure 3

ANISOTROPY DUE TO STRESS STATE

The initial kinetic fabric results in the anisotropy of elastic stiffness of a granular assembly if the force-dependent contact stiffness is adopted in equation (6). This type of material anisotropy is stress-induced.

Force-dependent contact stiffness

The contact stiffness can be assumed to be either contact-force independent (linear local constitutive law) or contact-force dependent (non-linear local constitutive law). The Hertz–Mindlin contact theory[30] constitutes a relation of the force-dependent contact stiffness. One may further take particle sliding and separation into account by imposing a local yielding condition on the contact point.[31] The Hertz–Mindlin contact theory is adopted

in the study. Based on this theory, the normal and shear contact stiffnesses take the following forms:

$$k_n = 1{\cdot}4423 \cdot G_s^{2/3} \cdot (1 - v_s)^{-2/3} \cdot (2 \cdot R_e)^{1/3} \cdot (f_n)^{1/3} \tag{20}$$

$$k_r = \lambda k_n = \left\{ \frac{2 \cdot (1 - v_s)}{2 - v_s} \left(\frac{f_r}{f_n \cdot \tan \phi_\mu} \right)^{1/2} \right\} \cdot k_n \tag{21}$$

where G_s and v_s are the elastic constants of particle solid; f_n and $f_r = \sqrt{f_s^2 + f_t^2}$ are the normal and shear contact-forces, respectively; ϕ_μ is the particle friction angle; and R_e is the equivalent relative radius. The terms f_n, f_s and f_t are the contact-force components acting at the contact point in the local co-ordinate system. The contact stiffness ratio λ is equal to $2(1 - v_s)/(2 - v_s)$ if local slippage at the contact region is ignored. The relative radius of each contact of spherical granular assembly, defined as $R = 1/(1/R_1 + 1/R_2)$, depends on the neighbouring particles sizes. R is equal to $r/2$ for an ideal granular assembly with the particle radius equal to r. In this study, a direction-dependent equivalent relative radius $R_e = (1/4) \cdot \ell$ is proposed to account for the effects of particle size, shape and preferred orientation of a non-ideal granular assembly on the contact stiffness. The contact stiffnesses calculated from equations (20)–(21) are stress dependent and non-linear. By adopting these equations for contact stiffness, equation (6) can capture the stress-induced anisotropy in the granular assembly once the contact-force distribution is known. The contact-force distribution in a granular assembly depends on the geometric fabric, local contact stiffness, and stress (or strain) history of the particulate assembly. For a non-ideal assembly (e.g., graded, non-spherical, random distributed, stress-dependent, etc.), it is hardly possible to obtain an exact (closed-form) solution of the contact-force distribution. The contact-force distribution, however, may be estimated by the method presented subsequently.

Estimation of contact-force distribution

It is possible to estimate the contact-force distribution in a representative volume by the concept of homogenization. Neglecting the angular deviation of branch vector and contact normal, the contact-force distribution $\overline{f}_j^{\tilde{n}}(\ell)$ can be estimated by the following equation (derived in the Appendix I):

$$\overline{f}_j^{\tilde{n}}(\ell) = \frac{1}{(M/V) \cdot \ell} \cdot \sigma_{pj} \cdot A_{p i_2 i_3 \ldots i_{2m}} \cdot n_{i_2} n_{i_3} \cdots n_{i_{2m}} \tag{22}$$

where $\overline{f}_j^{\tilde{n}}(\ell)$ is the contact force in the $\tilde{n}$ direction with a branch-vector length equal to ℓ; $\overline{f}_j^{\tilde{n}}(\ell) = \overline{f}_n^{\tilde{n}}(\ell) \cdot n_j + \overline{f}_s^{\tilde{n}}(\ell) \cdot s_j + \overline{f}_t^{\tilde{n}}(\ell) \cdot t_j$. The tensor $A_{p i_2 i_3 \ldots i_{2m}}$ is the inverse tensor of the first-kind fabric tensor of rank n; hence the relation $A_{p i_2 i_3 \ldots i_{2n}} \cdot N_{i i_2 i_3 \ldots i_{2m}} = \delta_{ip}$ holds.

For the fabric tensor of rank 2, equation (22) becomes

$$\overline{f}_j^{\tilde{n}}(\ell) = \frac{1}{(M/V) \cdot \ell} \cdot \sigma_{ij} \cdot A_{ik} \cdot n_k \tag{23}$$

where $A_{ik} \cdot N_{kq} = \delta_{iq}$. Equation (23) is identical with the static hypothesis for the ideal granular assembly proposed by Chang *et al.*[14] Kanatani[23] expresses the fabric tensor of the first kind in the form of $N_{ij} = \frac{2}{15} \cdot \delta_{ij} + \frac{1}{3} \cdot D_{ij}$; this tensor represents the sample mean of a directional data set, i.e. $N_{ij} = \int\int_\Omega n_i \cdot n_j \cdot E(\tilde{n})\, d\Omega$. Then, the tensor A_{ik} is equal to $(\frac{2}{15} \cdot \delta_{ik} + \frac{1}{3} \cdot D_{ik})^{-1}$. Equation (22) is a generalized form of the static hypothesis. As a result, equation (22) can account for the

anisotropy induced by the anisotropic stress state and can approximate the contact-force distribution. The calculation using equation (22) can only be regarded as an estimation of the exact contact force in a small strain condition. The estimated contact force is used to evaluate the stress-dependent local stiffness. It has to be pointed out that the real distribution of contact forces in a stressed granular assembly is stress path dependent and highly complicated.[52] The fomulation of the present micromechanics model is based on the kinematic hypothesis, while the estimation of contact force distribution is based on a static hypothesis. This aspect may result in a discrepancy of the estimated contact force and the real ones. Hence, equations (22)–(23) may not be generally applicable for complex stress (or strain) paths. For the sake of simplification, equation (23) is adopted in the parametric study. The estimated contact-force is utilized to evaluate the force-dependent local stiffness.

The anisotropy of the granular materials' mechanical behaviour can be categorized into (i) inherent anisotropy, and (ii) induced anisotropy. The inherent anisotropy is a physical characteristic inherent of a material independent of the applied strains. On the contrary, the induced anisotropy is a physical characteristic exclusively due to the strains associated with an applied stress state.[33,34] The presented model simulates the inherent anisotropy of natural granular materials by taking material's anisotropic microstructure into account; the anisotropic effect of geometric fabric is modelled by the anisotropic distributions of contact-normal and branch-vector length. On the other hand, the initial kinetic fabric (i.e. the anisotropic contact-force distribution) takes the effect of the anisotropic initial stress on the elastic stiffness into account. The subsequent section examines the effects of the microfeatures including geometric and kinetic fabric on the initial elastic stiffness of natural granular materials.

PARAMETRIC STUDY OF MICROFEATURES

In the following parametric study, the stress–strain relationship adopts the Voigt's notation, i.e. $\Delta\sigma_m = C_{mn}\cdot\Delta\varepsilon_n$, in which $\Delta\sigma_m = [\Delta\sigma_{11}, \Delta\sigma_{22}, \Delta\sigma_{33}, \Delta\tau_{12}, \Delta\tau_{13}, \Delta\tau_{23},]^{\mathrm{T}}$ is the stress increment vector and $\Delta\varepsilon_m = [\Delta\varepsilon_{11}, \Delta\varepsilon_{22}, \Delta\varepsilon_{33}, \Delta\gamma_{12}, \Delta\gamma_{13}, \Delta\gamma_{23},]^{\mathrm{T}}$ is the strain increment vector. Both m and n are tensor index (1–6). Figure 2 illustrates the global co-ordination system.

The effect of geometric fabric

The effects of gradation, shape, and preferred orientation on the elastic relation of a non-ideal particular assembly are demonstrated subsequently. To simplify microstructure description, the following assumptions are made in this sub-section.

(a) The contact-normal distribution function $E(\tilde{n})$ can be approximated by the third kind fabric tensor of rank two,[23] i.e. $E(\tilde{n}) = (1 + D_{rs}\cdot n_r\cdot n_s)/4\pi$.
(b) With an initial isotropic compression σ_c, the normal contact-force distributes uniformly and the shear contact-force does not exist.

In the following calculation for the parametric study, material parameters $\upsilon_s = 0{\cdot}21$, $G_s = 31$ Pa, and $e = 0{\cdot}5744$ are used. The average co-ordination number $\bar{N}^t$ is calculated from an empirical relationship $e = 1{\cdot}66 - 0{\cdot}125\cdot\bar{N}^t$, suggested by Chang *et al.*[35]

(1) *Effect of gradation*: Hypothetical granular assemblies composed of graded and randomly distributed spheres with branch-vector length distributions representing in the form of equation (14) are utilized for demonstrating the gradation effect. The packing structure and branch-vector-

length distributions are assumed isotropic; hence, equation (14) reduces to equation (15). The initial stiffness for the hypothetical assemblies presented in Figure 3 are calculated for $\sigma_c = 28$ kPa. For the assemblies corresponding to the curves 1–3 in Figure 3, the uniformity coefficients are identical ($C_u = 1{\cdot}9$) but their mean grain sizes are different. For assemblies corresponding to curves 4 ($C_u = 2{\cdot}9$), 5 ($C_u = 1{\cdot}9$) and 6 ($C_u = 1{\cdot}3$), the mean grain sizes are identical, but their uniformity coefficients are different. The calculated stiffness components for all the hypothetical assemblies are $C_{33} = C_{11} = C_{22} = 5465$ MPa, $C_{44} = C_{55} = C_{66} = 2665$ MPa, and $C_{13} = C_{23} = C_{12} = 134$ MPa, despite the difference in either uniformity or mean grain size.

The above results reveal a few phenomena. First, it appears that the initial stiffness of a granular assembly with a constant void ratio remains unchanged even with different mean grain sizes. Chang *et al.*[27] also find that the elastic stiffness of an ideal granular assembly is independent of the particle size if the Hertz contact theory is adopted in a micromechanics-based model. Second, the initial elastic stiffness is independent of the uniformity of granular assembly in case that e and $\bar{N}^t$ remain constant. This argument is supported by the experimental data of Iwasakiand Tatsuoka.[36] Their data comes from the resonant-column tests on uniform clean sand (with $1{\cdot}31 < C_u < 1{\cdot}80$ and $0{\cdot}162$ mm $< D_{50} < 3{\cdot}2$ mm). Iwasaki and Tatsuoka[36] report that the particle size and gradation have little effect on the dynamic shear modulus (eiquivalent to the initial shear modulus) of sands. Since $\bar{N}^t$ correlates very well with the void ratio and does not depend on the grain-size distribution,[26] it can be argued tht the primary effect of gradation (on the dynamic shear modulus) arises from its influence on the void ratio which largely affects the magnitude of the stiffness tensor. Chang *et al.*[35] demonstrated the similar effect of void ratio on the dynamic shear modulus.

It should be noted that the presented model does not consider the deformation mechanism of a gap-graded granular assembly (such as bimodal particle size distribution). Nor does it take clay-sized fines contained in an assembly into account.

(2) *Effects of shape and preferred orientation*: Hypothetical non-spherical assembly with a branch-vector length distribution represented in a special form of equation (14) is used to study the effects of particle's shape and preferred orientation. The function $g^{\tilde{n}}(\ell)$ accounts or the effects of the particle shape and preferred orientation. For a mono-sized non-spherical assembly, there is no fluctuation of branch-vector length along $\tilde{n}$. Hence, $g^{\tilde{n}}(\ell)$ can be represented as a Dirac delta function,[15] such as $g^{\tilde{n}}(\ell) = \delta(\ell - \bar{\ell}_e \cdot W^r(\tilde{n}))$, in which $W^r(\tilde{n}) = (1 + D^r_{rs} \cdot n_r \cdot n_s)$ is a weighting function reflecting the combined effects of particles' flatness and preferred orientation; D^r_{rs} is a third kind fabric tensor of rank two; $\bar{\ell}_e$ is the equivalent (averaged) branch-vector length. For a horizontally deposited granular material, the direction-dependent weighting function $W^r(\tilde{n}) = (1 + D^r_{rs} \cdot n_r \cdot n_s)$ is transversely isotropic; it requires $D^r_{ij} = 0$ for $i \neq j$ and $2D^r_{11} = 2D^r_{22} = -D^r_{33}$. Figures 5(a)–5(d) are the three-dimensional plots of the direction-dependent weighting functions approximated by various fabric tensors D^r_{ij}. Figure 5(a) ($D^r_{33} = 0$) displays a uniform (isotropic) distribution of average branch-vector length. In the cases corresponding to Figure 5(b) ($D^r_{33} = -0{\cdot}3$), Figure 5(c) ($D^r_{33} = -0{\cdot}6$), and Figure 5(d) ($D^r_{33} = -0{\cdot}9$), the average branch-vector length along the horizontal direction is longer than that along the vertical direction (implying that the preferred orientation of the particles' long axis is along the horizontal direction). The direction-dependent weighting functions in Figure 5(a)–(d) represent mono-sized granular assemblies with various particles' flatness and preferred orientation. Figure 5(e) shows a transversely isotropic distribution function $E(\tilde{n}) = (1 + D_{rs} \cdot n_r \cdot n_s)/4\pi$ of contact normal with the fabric tensor $D_{33} = 0{\cdot}3$.

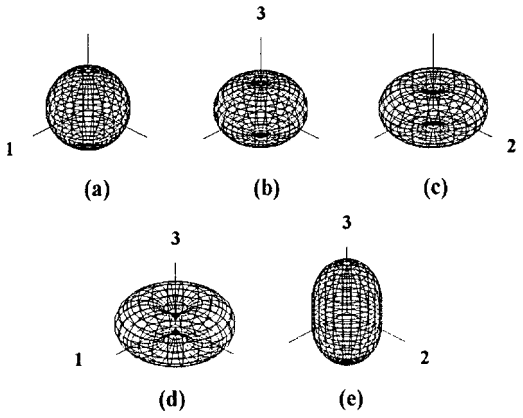

Figure 5. (a)–(d) Weighting function $W(\tilde{n})$ for (a) $D^r_{33} = 0$; (b) $D^r_{33} = -0{\cdot}3$; (c) $D^r_{33} = -0{\cdot}6$; (d) $D^r_{33} = -0{\cdot}9$; (e) Distribution of contact normal $E(\tilde{n})$ for $D_{33} = 0{\cdot}3$

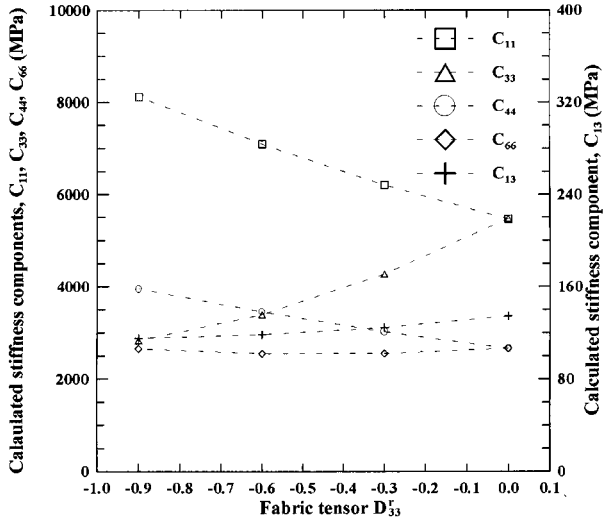

Figure 6. Calculated stiffness components versus fabric tensor D^r_{33}

The distribution of the branch-vector length in various directions implicitly takes the effects of shape and preferred orientation into account. Figure 6 illustrates the influence of anisotropic distribution of branch-vector length on the elastic stiffness of granular assemblies. The packing structure of the assembly is assumed isotropic. Despite of isotropic packing structure and stress state (= 28 kPa), it is noted that the degree of anisotropy correlates with the anisotropy resulted from the combined effects of shape and preferred orientation. The effect of geometric fabric (including packing structure and branch-vector length distributions) is shown in Table II. The degree of anisotropy is evaluated by the stiffness ratio C_{11}/C_{33} and C_{66}/C_{44}. C_{11} and C_{33} are the normal stiffness on the horizontal plane and vertical plane, respectively; C_{66} and C_{44} are

Table II. The effect of geometric fabric on the stiffness ratio (ignoring kinetic fabric)

	Components of fabric tensors describing the packing structure and distribution of branch-vector length	Stiffness ratio C_{11}/C_{33}	Stiffness ratio C_{66}/C_{44}
Case 1	$D_{33} = 0{\cdot}0$, $D^r_{33} = -0{\cdot}3$	1·452	0·845
Case 2	$D_{33} = 0{\cdot}3$, $D^r_{33} = 0{\cdot}0$	0·833	1·099
Case 3	$D_{33} = 0{\cdot}3$, $D^r_{33} = -0{\cdot}3$	1·226	0·909

Table III. Effect of kinetic fabric on the stiffness ratio (for $D_{33} = 0{\cdot}3$, $D^r_{33} = -0{\cdot}3$)

	Conditions	Stiffness ratio C_{11}/C_{33}	Stiffness ratio C_{66}/C_{44}
Case 1	Kinetic fabric is isotropic	1·226	0·909
Case 2	Kinetic fabric is considered, no local partial slippage	1·254	0·900
Case 3	Kinetic fabric is considered, with local partial slippage	1·279	0·902

the shear-stiffness component on the vertical plane and horizontal plane, respectively. It is noted in case 1 of Table II that the stiffness ratio C_{11}/C_{33} of a granular assembly with isotropic packing is larger than 1·0 if the distribution of the branch-vector length is anisotropic and the major principal plane is horizontal. As seen in case 3 of Table II, a packing structure even with more contact normal in the vertical direction can still have higher stiffness in the horizontal direction as long as the branch-vector length is longer in the horizontal direction. Using the presented statistical description of microstructure, the calculated shear wave velocity propagating along the horizontal direction is higher than the shear wave velocity along all other directions.[15] This trend satisfactorily agrees with the experimental evidence,[37] quantitatively. It also demonstrates the appropriateness of using two separate fabric tensors, D_{ij} and D^r_{ij}, respectively, to account for the contact normal distribution and the branch-vector length distribution of a non-spherical granular assembly. Statistical expressions of these distributions can reasonably account for the random nature of a realistic granular material.

The effect of kinetic fabric

The kinetic fabric (contact-force distribution) results in the stress-induced anisotropy in initial stiffness. The initial kinetic fabric is a function of microstructure and the initial stress state of granular assembly (noticeable from equations (22)–(23)). A demonstration and discussion of the effect of kinetic fabric on the elastic stiffness of granular assembly follow. Two cases are discussed, they are (1) anisotropic geometric fabric under isotropic stress state and (2) isotropic geometric fabric under anisotropic stress state. Assumptions (a) and (b) in the last sub-section remains in the following demonstration.

(1) *Isotropic stress state with anisotropic geometric fabric*: To begin with, Table III demonstrates the effect of kinetic fabric assuming the same microstructure of the granular assembly in the case 3 of Table II. The granular assembly has the packing structure as Figure 5(e) and the

density function accounting for the effects of shape and preferred orientation as Figure 5(b). The isotropic confining stress is 28 kPa and the friction angle ϕ_μ is 12°. In case 2 of Tables III local partial slippage at the contact region is ignored (i.e. no consideration on the reduction in the shear contact stiffness due to the contact shear) for calculating the stiffness ratio λ. By comparing cases 1 and 2 of Table III, it is noted that the degree of anisotropy is slightly higher when the kinetic fabric is considered. Case 3 of Tables III shows the initial stiffness ratio when local partial slippage is considered. It can be noted from equation (21) that the shear contact stiffness decreases

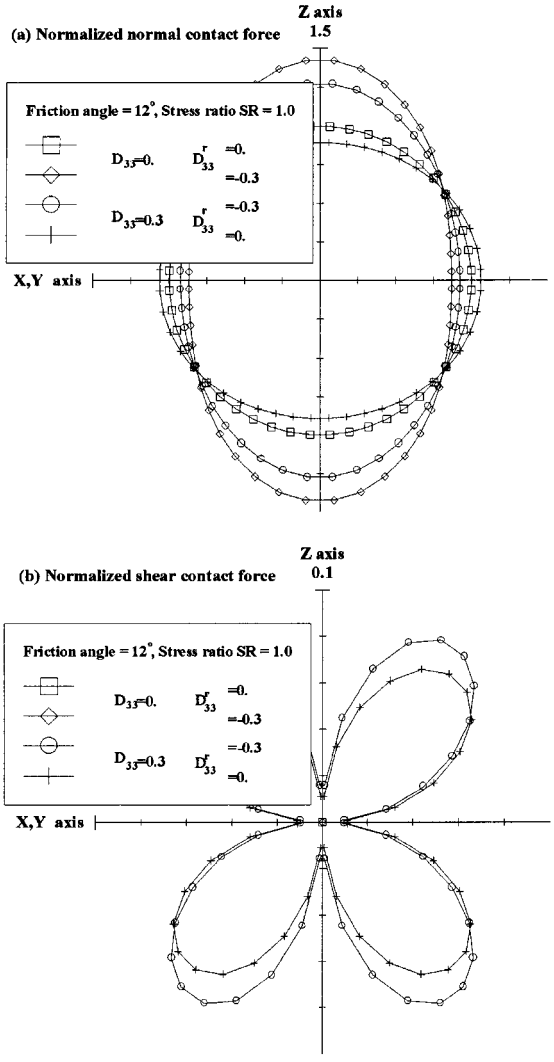

Figure 7. (a) Normal contact-force distribution for granular assemblies with different D_{33} and D^r_{33}. (b) Shear contact-force distribution for granular assemblies with different D_{33} and D^r_{33}. (c) Normal contact-stiffness distribution for granular assemblies with different D_{33} and D^r_{33}. (d) Shear contact-stiffness distribution for granular assemblies with different D_{33} and D^r_{33}

as local partial slippage occurs. The local partial slippage in the contact region obviously influences the degree of anisotropy.

The normal and shear contact force are normalized by $\bar{f}_n^o (= 3 \cdot V \cdot \sigma_c / 2 \cdot r \cdot M)$ (i.e. the normal force for an ideal assembly subjected to an isotropic stress σ_c) in order to demonstrate the kinetic anisotropy of granular assembly. Figures 7(a) and 7(b) present the distribution of the normalized normal and shear contact force for various microstructures. The kinetic fabric is anisotropic despite of the isotropic stress state. It is noted in Figure 7(b) that no shear contact force exists for isotropic packing structure. The influence of kinetic fabric on the contact stiffness is also demonstrated. The normal and shear contact stiffnesses are normalized by $k_n = 1{\cdot}4423 \cdot G_s^{2/3} \cdot (1 - v_s)^{-2/3} \cdot r^{1/3} \cdot (\bar{f}_n^o)^{1/3}$ (i.e. the normal contact stiffness for an ideal assembly subjected to

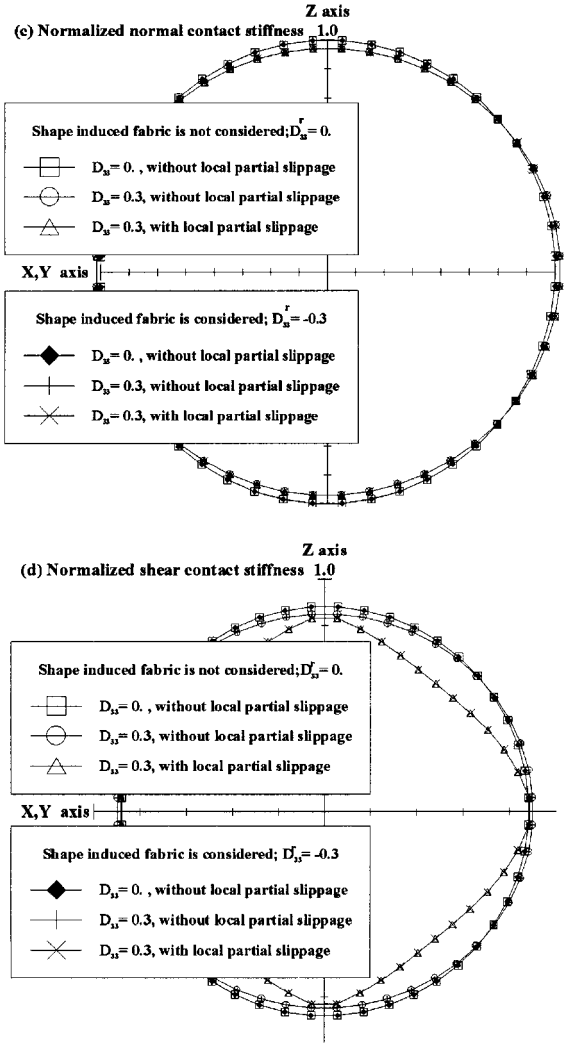

Figure 7. (continued)

isotropic stress σ_c). Figure 7(c) compares the normalized normal contact-stiffness distribution of the granular assemblies with various microstructures. It shows that the normal contact stiffness is hardly influenced by the shape-induced fabric, D_{33}^r, regardless of what has the local partial slippage is considered or not Figure 7(d) shows that the local slippage at the contact region has a reducing effect on the normalized shear contact stiffness.

Figures 8(a)–(d) demonstrate the effect of kinetic fabric clearly. These figures present the distribution of normalized contact force and contact stiffness of an ideal granular assembly with anisotropic packing structure under isotropic stress state. It is noted in Figure 8(a) that the

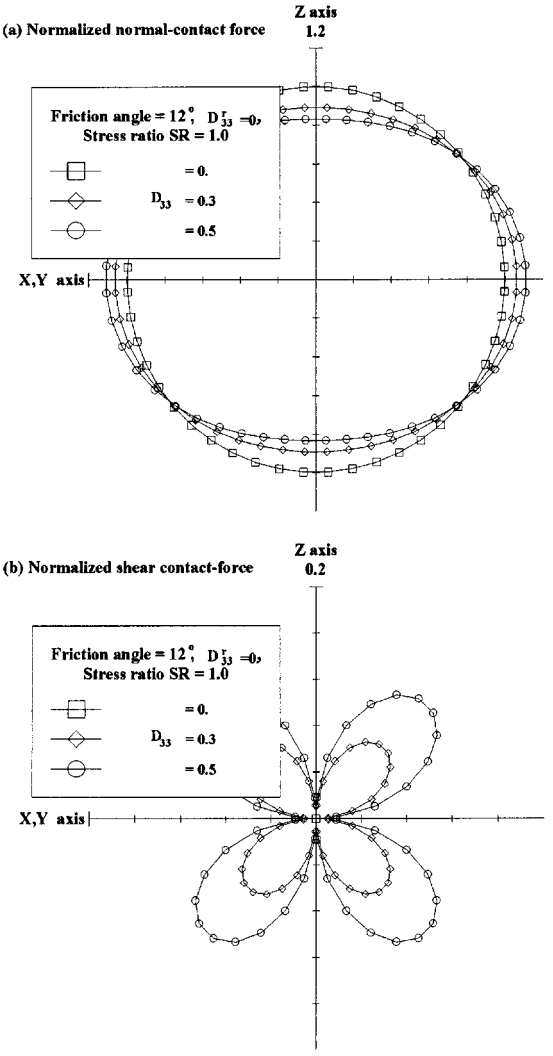

Figure 8. (a) Normal contact-force distribution for ideal granular assemblies with different D_{33} under isotropic stress. (b) Shear contact-force distribution for ideal granular assemblies with different D_{33} under isotropic stress. (c) Normal contact-stiffness distribution for ideal granular assemblies with different D_{33} under isotropic stress. (d) Shear contact-stiffness distribution for ideal granular assemblies with different D_{33} under isotropic stress

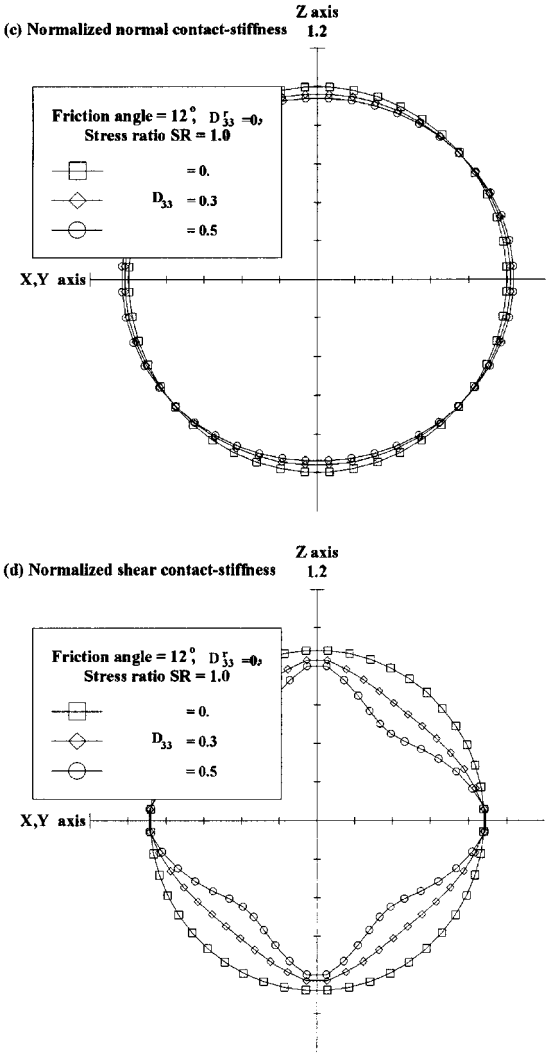

Figure 8. (continued)

distribution of normalized normal contact force is not isotropic even under an isotropic stress state. The more contact normal distributed in the vertical direction, the less the contact force needs to be shared for each contact point. The normalized shear contact force of granular assembly increases with the increasing degree of anisotropy in packing structure, which is shown in Figure 8(b). The normalized normal and shear contact stiffnesses are shown in Figures 8(c) and (d), respectively. Table IV lists the stiffness ratio of the three different packing structures. It illustrates that the anisotropy of deformation increases with an increasing D_{33}.

(2) *Anisotropic stress state with isotropic geometric fabric*: The effect of the anisotropic stress state on the elastic stiffness of an ideal granular assembly with isotropic geometric fabric is further

Table IV. Effect of packing structure on stiffness ratio of ideal granular assembly under isotropic confining pressure

Components of fabric tensors	Stiffness ratio C_{11}/C_{33}	Stiffness ratio C_{66}/C_{44}
$D_{33} = 0{\cdot}0$	1·000	1·000
$D_{33} = 0{\cdot}3$	1·857	1·091
$D_{33} = 0{\cdot}5$	1·744	1·160

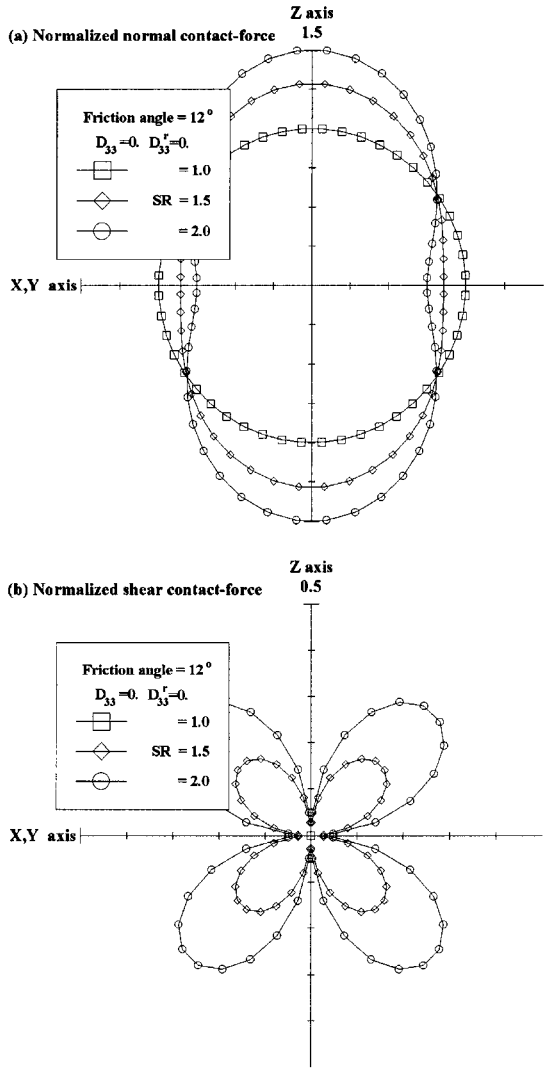

Figure 9. (a) Normal contact-force distribution for ideal granular assemblies with isotropic packing structure under anisotropic stress. (b) Shear contact-force distribution for ideal granular assemblies with isotropic packing structure under anisotropic stress. (c) Normal contact-stiffness distribution for ideal granular assemblies with isotropic packing structure under anisotropic stress. (d) Shear contact-stiffness distribution for ideal granular assemblies with isotropic packing structure under anisotropic stress

studied. The friction angle ϕ_μ is also set 12° in the following illustration. The assembly's packing structure is assumed isotropic. Figures 9(a) and (b) show the influence of anisotropic stress state on the normalized contact forces. An anisotropic initial stress state tends to induce an anisotropic distribution of the normal and shear contact forces. The stress ratio (SR) in Figure 9 is defined as the major principal stress over minor principal stress, i.e. σ_{33}/σ_{11} ($\sigma_{11} = \sigma_{22}$, under a biaxial condition). The first invariant of stress tensor $I_1 = (\sigma_{33} + 2\sigma_{11})/3$ remains constant. The higher the stress ratio (SR), the more concentration of normal contact force in the major principal direction. The pattern of normal and shear contact-for distribution agrees with the DEM simulated results.[3] The resulting normalized contact stiffness is anisotropic (see Figures 9(c) and

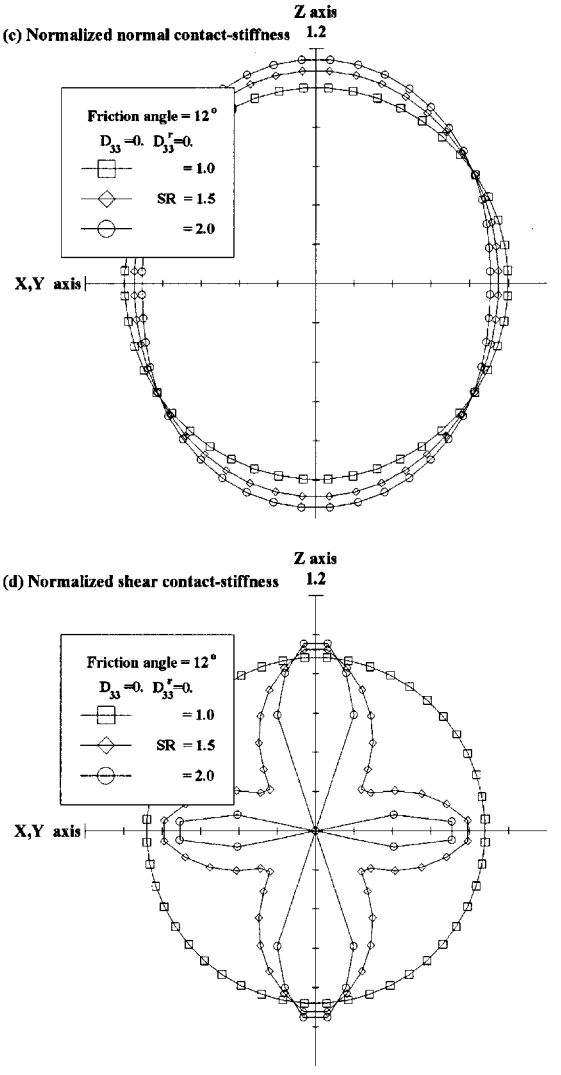

Figure 9. (continued)

Table V. Effect of stress ratio on stiffness ratio of ideal granular assembly

Stress ratio SR	Stiffness ratio C_{11}/C_{33}	Stiffness ratio C_{66}/C_{44}
1·0	1·000	1·000
1·5	0·972	1·082
2·0	0·940	1·181

(d)) according to equations (20 and (21). The initial stiffness of an ideal granular assembly is also anisotropic for an anisotropic initial stress state. Table V lists the stiffness ratio of the three different stress ratio SR. It shows that the anisotropy of deformation increases with an increasing SR.

SUMMARY AND CONCLUSIONS

This paper presents a micromechanics model for the elastic stiffness of a non-spherical granular assembly. The microstructural continuum model of the ideal assemblies[7] is extended for non-ideal assemblies. The presented model implicitly takes the effects of gradation, shape, and preferred orientation into account by a direction-dependent branch-vector length distribution function. The microstructure of the granular assembly is described by the distributions of packing structure, branch-vector length, and particle number per unit volume. Statistical expressions of these microfeatures account for the random nature of realistic granular materials. The microfeatures relevant to the description of non-spherical particulate assembly are elaborated. The influences of various direction-dependent and direction-independent microfeatures on the elastic stiffness are demonstrated. Hypothetical granular assemblies are used to study the effects of gradation, shape, and preferred orientation. Based on the proposed model incorporating two separate fabric tensors, the paper discusses the inherent anisotropy of a non-spherical granular assembly.

The presented work also makes use of a generalized static hypothesis to estimate the contact-force distribution for specific microstructure and stress state. With the estimated contact force and the Hertz–Mindlin contact theory, the elastic stiffness of a particulate assembly can be evaluated. Hence, the effects of geometric fabric and anisotropic stress state on the elastic stiffness can be deliberated. Consequently, the inherent anisotropy and the stress-nduced anisotropy of a natural granular material under small strain can be evaluated independently.

It is shown that the proposed model can reasonably capture the phenomena of inherent anisotropy and stress-induced anisotropy of a non-spherical granular assembly under small strain. Application of the proposed model on natural granular materials appears promising.[15]

ACKNOWLEDGEMENTS

This work was financially supported by the National Science Council of the Republic of China. This support is gratefully acknowledged.

APPENDIX I

Proof of the generalized kinetic hypothesis

The average stress σ_{ij} can be obtained by summing the product of individual contact-force f_j^c and branch vector ℓ_i^c (at the cth contact) on the basis of equilibrium condition[9] or virtual work theory[6] as follows:

$$\sigma_{ij} = \frac{1}{V} \sum_{c=1}^{M} \ell_i^c \cdot f_j^c \tag{24}$$

Introducing the density function of contact-normal and branch-vector length distribution and rewriting in an integral form, equation (24) becomes

$$\sigma_{ij} = \frac{2 \cdot M}{2 \cdot V} \iint_{\Omega} \left(\int g^{\tilde{n}}(\ell) \cdot \ell_i^c \cdot f_j^c \, \mathrm{d}\ell \right) \cdot E(\tilde{n}) \, \mathrm{d}\Omega \tag{25}$$

Ignoring the angular deviation of branch vector and contact normal (i.e. $n_i^{\ell} = n_i^c = n_i$), the following equation holds:

$$\begin{aligned} &\frac{2 \cdot M}{2 \cdot V} \iint_{\Omega} \left(\int g^{\tilde{n}}(\ell) \cdot \ell_i \cdot f_j^c \, \mathrm{d}\ell \right) \cdot E(\tilde{n}) \, \mathrm{d}\Omega \\ &= \frac{2 \cdot M}{2 \cdot V} \iint_{\Omega} \left(\int g^{\tilde{n}}(\ell) \cdot \ell_i \left(\frac{1}{\left(\frac{2 \cdot M}{2 \cdot V} \cdot \ell \right)} \sigma_{pj} \cdot A_{p i_2 i_3 \ldots i_{2m}} \cdot n_{i_2} n_{i_3} \cdots n_{i_{2m}} \right) \mathrm{d}\ell \right) \cdot E(\tilde{n}) \, \mathrm{d}\Omega \\ &= \iint_{\Omega} \left(\int g^{\tilde{n}}(\ell) \cdot n_i \cdot (\sigma_{pj} \cdot A_{p i_2 i_3 \ldots i_{2m}} \cdot n_{i_2} n_{i_3} \cdots n_{i_{2m}}) \, \mathrm{d}\ell \right) \cdot E(\tilde{n}) \, \mathrm{d}\Omega \end{aligned} \tag{26}$$

If the item $\sigma_{pj} \cdot A_{p i_2 i_3 \ldots i_{2m}} \cdot n_{i_2} n_{i_3} \cdots n_{i_{2m}}$ does not depend on the branch-vector length, the following equation holds:

$$\begin{aligned} &\int g^{\tilde{n}}(\ell) \cdot n_i \cdot (\sigma_{pj} \cdot A_{p i_2 i_3 \ldots i_{2m}} \cdot n_{i_2} n_{i_3} \cdots n_{i_{2m}}) \, \mathrm{d}\ell \\ &\quad = \left(\int g^{\tilde{n}}(\ell) \cdot \mathrm{d}\ell \right) \cdot (\sigma_{pj} \cdot A_{p i_2 i_3 \ldots i_{2m}} \cdot n_{i_2} n_{i_3} \cdots n_{i_{2m}}) \cdot n_i \\ &\quad = (\sigma_{pj} \cdot A_{p i_2 i_3 \ldots i_{2m}} \cdot n_{i_2} n_{i_3} \cdots n_{i_{2m}}) \cdot n_i \end{aligned} \tag{27}$$

Substituting equation (27) into equation (26), equation (26) then becomes

$$\begin{aligned} &\frac{2 \cdot M}{2 \cdot V} \iint_{\Omega} \left(\int g^{\tilde{n}}(\ell) \cdot \ell_i \cdot f_j^c \, \mathrm{d}\ell \right) \cdot E(\tilde{n}) \, \mathrm{d}\Omega \\ &\quad = \iint_{\Omega} (\sigma_{pj} \cdot A_{p i_2 i_3 \ldots i_{2m}} \cdot n_{i_2} n_{i_3} \cdots n_{i_{2m}}) \cdot n_i \cdot E(\tilde{n}) \, \mathrm{d}\Omega \\ &\quad = \sigma_{pj} \cdot A_{p i_2 i_3 \ldots i_{2m}} \cdot \left[\iint_{\Omega} n_{i_2} n_{i_3} \cdots n_{i_{2m}}) \cdot n_i \cdot E(\tilde{n}) \, \mathrm{d}\Omega \right] \\ &\quad = \sigma_{pj} \cdot A_{p i_2 i_3 \ldots i_{2m}} \cdot N_{i i_2 i_3 \ldots i_{2m}} \end{aligned} \tag{28}$$

If $A_{p i_2 i_3 \ldots i_n} \cdot N_{i i_2 i_3 \ldots i_n} = \delta_{ip}$, equation (25) is satisfied. Hence, equation (22) can estimate the contact-force distribution.

APPENDIX II

Notation

A, A'	constants
$A_{ik}, D_{rs}, D'_{mn}, N_{ij}$	fabric tensors of rank-two
$A_{p i_2 i_3 \dots i_n} \cdot N_{i i_2 i_3 \dots i_n}$	fabric tensors of tank-n
C_{ijkl}	elastic stiffness tensor
C_{mn}	elastic stiffness tensor in Voigt' notation
$E(\tilde{n})$	density function of contact normal
e	void ratio
$F(r)$	gradation function
$f^v(r), f^p(r)$	grain size density function by volume and particle number
$\bar{f}_j^{\tilde{n}}(\ell)$	averaged contact-force tensor in $\tilde{n}$ direction
$\bar{f}_n^o$	averaged normal contact force in a granular assembly
f_n, f_s, f_t	contact-force components in the n, s, t direction
f_r	shear contact force
G_s	shear modulus of particle solids
$g^{\tilde{n}}(\ell)$	branch-vector length distribution function
$g(\ell), g^{\text{total}}(\ell)$	direction-independent distribution function of ℓ
I_{pqik}	identical tensor
I_1	first invariant of stress tensor
k_{jl}^c	contact stiffness tensor in 'cth' contact
k_n^c, k_s^c, k_t^c	contact stiffnesses in the n, s, t direction in 'cth' contact
k_n, k_r	normal and shear contact stiffnesses
ℓ_i^c, ℓ^c	branch-vector tensor and the 'cth' branch-vector length
$\bar{\ell}_{50}^{\tilde{n}}, \ell_{50}$	sample mean of branch-vector length
$\bar{\ell}_e$	equivalent (averaged) branch-vector length
M	total contact number in the volume
$N^{\tilde{n}}, N^{\tilde{n}^a}$	contact number in the $\tilde{n}$ and $\tilde{n}^a$ direction
$N_\ell^{\tilde{n}}, N_\ell^{\tilde{n}^a}$,	contact number in the $\tilde{n}$ and $\tilde{n}^a$ direction with branch-vector length $= \ell$
$\bar{N}^t$	average co-ordination number
$\tilde{n}; n_i^c, s_i^c, t_i^c$,	unit vectors and tensors of the local co-ordinate system
$n_i^{\ell^c}$	unit branch vector
P^v	total particle number in the volume V
R, R_e	relative radius and equivalent relative radius
r, r_e	particle radius and equivalent radius
r_m, r_M	minimum and maximum of particle radius
$r_{50}^{\tilde{n}}, r_{50}$	sample means of radius
r_{pqik}	deviation tensor
s_r, s_ℓ	standard deviations of $f^v(r)$ and $g(\ell)$
$s_r^{\tilde{n}}, s_\ell^{\tilde{n}}$	direction-dependent standard deviations
V	representative volume of the granular assembly
$V_s, v_s(r)$	volume of solid and volume of a particle with the size r
$W(\tilde{n}), W^r(\tilde{n})$	direction dependent weighting functions

Greek letters

δ^v	the total particle number per unit volume
δ_{ij}	Kronecker delta tensor
ϕ_μ	inter-particle frictional angle
υ_s	Poisson's ratio of particle solid
λ	stiffness ratio
ρ	particle diameter
σ_c	isotropic confining stress
σ_{ij}, ε_{ij}	stress and strain tensors
$\Delta\sigma_m$, $\Delta\varepsilon_n$	incremental stress and strain tensors in Voigt' notation
Ω, $d\Omega$	unit sphere, and elementary angle

REFERENCES

1. P. A. Cundal and O. D. L. Strack, 'A discrete numerical model for granular assemblies', *Geotechnique*, **29**(1)**,** 47–65 (1979).
2. Y. Kishino, 'Disc model analysis of granular media', in M. Satake and J. T. Jenkins (eds), *Micromechanics of Granular Materials*, Elsevier, Amsterdam, The Netherland, 1988, pp. 143–152.
3. L. Rothenburg and R. J. Bathurst, 'Micromechanical features of granular assemblies with planar eliptical particles', *Geotechnique*, **4**(1)**,** 79–95 (1992).
4. T. T. Ng, 'Numerical simulations of granular soil using eliptical particles', *Comput. Geotech.l*, **16,** 153–169 (1994).
5. T.-C. Ke and J. Bray, 'Modeling of particulate media using discontinuous deformation analysis, *J. Engng. Mech. ASCE*, **121**(11)**,** 1234–1243 (1995).
6. J. Christoffersen, M. M. Mehrabadi and S. Nemat-Nasser, 'A micromechanical description of granular material behavior', *J. Appl. Mech. ASME*, **48**(2)**,** 339–344 (1981).
7. C. S. Chang, 'Micromechanical modelling of constitutive relations for granular material', in M. Satake and J. T. Jenkins (eds), *Micromechanics of Granular Materials*, Elsevier, Amsterdam, The Netherland, 1988, pp. 271–278.
8. R. J. Bathurst and L. Rothenburg, 'Micromechanical aspects of isotropic granular assemblies with linear contact interactions', *J. Appl. Mech. ASME*, **55**(1)**,** 17–23 (1988).
9. C. S. Chang and A. Misra, 'Theoretical and experimental study of regular packings of granules', *J. Engng. Mech. ASCE*, **115**(4)**,** 704–720 (1989).
10. B. Cambou, 'From global to local variable in granular materials', in Thornton (ed.), *Podwers & Grains 93*, 1993, pp. 73–86.
11. P. Emeriault and B. Cambou, 'Micromechanical modelling of anisotropic non-linear elasticity of granular medium', *Int. J. Solids Struc.* **33**(18)**,** 2591–2607 (1996).
12. C. S. Chang and A. Misra, 'Application of uniform strain theory to heterogeneous granular solids', *J. Engng. Mech. ASCE*, **116**(10)**,** 2310–2328 (1990).
13. C. S. Chang and A. Misra, 'Packing structure and mechanical properties of granulates', *J. Engng. Mech., ASCE*, **116**(5)**,** 1077–1093 (1990).
14. C. S. Chang, S. J. Chao and Y. Chang, 'Estimates of elastic moduli for granular material with anisotropic random packing structure', *Int. J. Solids Struc.*, **32**(14)**,** 1989–2008 (1995).
15. Y. W. Pan and J. J. Dong, 'A Novel Methodology for Evaluating the Fabric of Granular Material', *Geotechnique*, Accepted (1999).
16. M. Oda, 'The mechanism of fabric changes during compressional deformation of sand, *Soils Found.*, **12**(2)**,** 1–18 (1972).
17. M. Oda, S. Nemat-Nasser and J. Konishi, 'Stress-induced anisotropic in granular masses', *Soils Found.*, **25**(3)**,** 85–97 (1985).
18. Y. C. Chen, I. Ishibashi and J. T. Jenkings, 'Dynamic shear modulus and fabric: part I, depositional and induced anisotropy', *Geotechnique*, **38**(1)**,** 25–32 (1988).
19. C. S. Chang, M. G. Kabir and Y. Chang, 'Micromechanics modelling for stress-strain behavior of granular soils II: evaluation, *J. Geotech. Engng. ASCE*, **118**(12)**,** 1975–1992 (1992).
20. M. M. Mehrabadi, B. Loret and S. Nemat-Nasser, 'Incremental constitutive relations for granular materials based on micromechanics', *Proc. Roy. Soc. London A*, **441,** 433–463 (1993).
21. M. H. Sadd, J. Gao and A. Shukla, 'Numerical analysis of wave propagation through assemblies of eliptical particles', *Comput. Geotech.*, **20**(3)**,** 323–343 (1997).

22. M. Oda, S. Nemat-Nasser and M. M. Mehrabadi, 'A statistical study of fabric in an random assembly of spherical granules', *Int. J. Numer. Anal. Meth. Geomech.*, **6**(1), 77–94 (1982).
23. K. Kanatani, 'Distribution of directional data and fabric tensors', *Int. J. Engng. Sci.*, **22**(2), 149–164 (1984).
24. M. Oda, 'Geometry of discontinuity and its relation to mechanical properties of discontinuous materials', in P. A. Vermeer and H. J. Luger (eds), *Proc., IUTAM Symp. on Deformation and Failure of Granular Materials*. A.A. Balkema, Delft, The Netherlands, 1982, pp. 63–68.
25. M. Satake, 'Fabric tensor in granular materials', in P. A. Vermeer and H. J. Luger (eds), *Proc., IUTAM Symp. on Deformation and Failure of Granular Materials*. A. A. Balkema, Delft, The Netherlands, 1982, pp. 63–68.
26. M. Oda, 'Co-ordination number and its relation to shear strength of granular material', *Soils Found.*, **17**(2), 29–42 (1977).
27. C. Chang, S. S. Sundaram and A. Misra, 'Initial moduli of particulates mass with frictional contacts', *Int. J. Numer. Anal. Meth. Geomech.*, **13**(6), 626–641 (1989).
28. J. Feda, *Mechanics of Particulate Materials*, Elsevier Scientific Publishing Company, Amsterdam, 1982.
29. C. R. G. Treasure, 'Powers and granular solid: the examination and description of particulate components', in J. C. Richards (ed.), *The Storage and Recovery of Particulate Solids*, Inst. of Chem. Engng., London, 1966, pp. 21–37.
30. R. D. Mindlin, 'Compliance of elastic bodies in contact', *J. Appl. Mech., ASME*, **13**(3), 259–268 (1949).
31. C. S. Chang, Y. Chang and M. G. Kabir, 'Micromechanics modelling for stress-strain behavior of granular soils I: theory', *J. Geotech. Engng.*, **118**(12), 1959–1974 (1992).
32. Y. C. Chen and H. Y. Hung, 'Evolution of shear modulus and fabric during shear deformation', *Soils Found.*, **31**(4), 148–160 (991).
33. A Casagrande and N. Carillo, 'Shear failure of anisotropic materials', *Proc. Boston Soc. Civil Engrs.*, **31,** 74–87 (1994).
34. J. R. F. Arthur and B. K. Menzies, 'Inherent anisotropic in a sand', *Geotechnique*, **22**(1), 115–128 (1972).
35. C. S. Chang, A. Misr and S. S. Sundaram, 'Properties of granular packing under low amplitude cyclic loading', *Int. J. Soil Dyn. Earthquake Engng.*, **10**(4), 201–211 (1991).
36. T. Iwasaki and F. Tatsuoka, 'Effects of grain size and grading on dynamic shear moduli of sands', *Soils Found.*, **17**(1), 19–35 (1977).
37. S. H. H. Lee and K. H., II Stokoe, 'Investigation of low-amplitude shear wave velocity in anisotropic material', *Report GR84-6*, Civil Engineering Department, University of Texas at Austin, 1986.

